Science Advances
AAAS

Supplementary Materials for

pH regulates potassium conductance and drives a constitutive proton current in human TMEM175

Wang Zheng, Chen Shen, Longfei Wang, Shaun Rawson, Wen Jun Xie, Carl Nist-Lund, Jason Wu, Zhangfei Shen, Shiyu Xia, Jeffrey R. Holt*, Hao Wu*, Tian-Min Fu*

*Corresponding author. Email: jeffrey.holt@childrens.harvard.edu (J.R.H.); wu@crystal.harvard.edu (H.W.); fu.978@osu.edu (T.-M.F.)

Published 25 March 2022, *Sci. Adv.* **8**, eabm1568 (2022)
DOI: 10.1126/sciadv.abm1568

This PDF file includes:

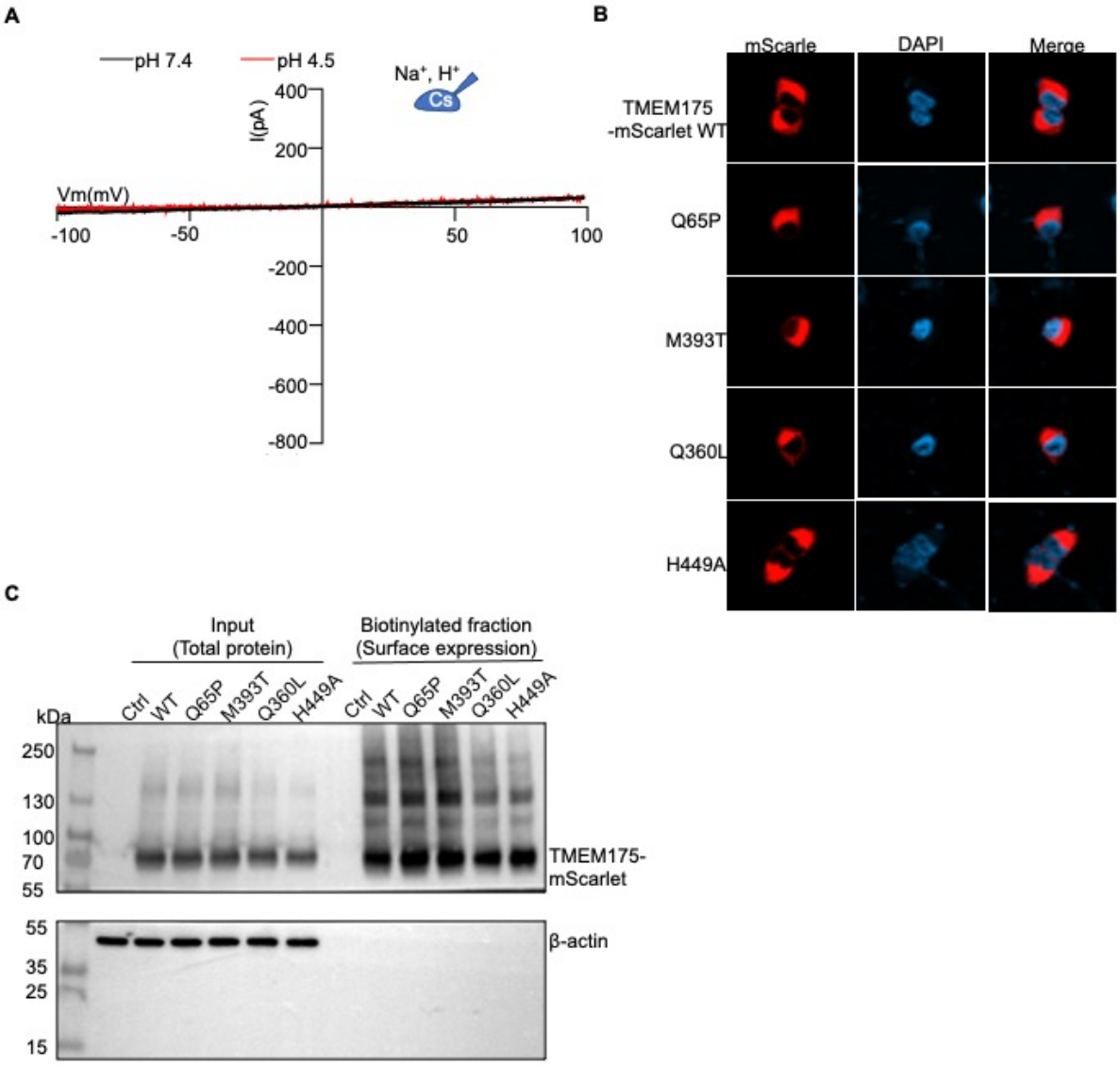

Fig. S1. Expression of TMEM175 wild type and mutants

(A) Representative current-voltage (*I-V*) curves obtained in whole-cell configuration from non-transfected HEK293T cells. The pipette solution contains 150 mM Cs^+, and 150 mM Na^+ was used in the bath solution.

(B) Confocal microscopy images of TMEM175-mScarlet wild type and mutants in HEK293T cells, showing the expression and localization of TMEM175.

(C) Western blot analysis of TMEM175 wild type and mutants, showing similar expression levels of wild type and mutants.

Fig. S2. Proton conductance by human TMEM175

(A) Representative fluorescence images of pHrodo Green in HEK293T cells before and after low pH perfusion. HEK293T cells express either wild-type TMEM175, two mutant TMEM175 proteins Q360L and I271W with increased and decreased proton conductance, respectively, and sham lipofectamine only transfected cells as indicated. Transfected HEK293T cells expressing the channel of interest were confirmed via fluorescence in the mCherry channel. Scale bar 50 μm.

(B) Time-lapse fluorescence emission intensity calculated as $\Delta F/F_0$ over the course of 15 minutes. The first 30 seconds were used to determine the baseline fluorescence before 14.5 minutes of perfusion of pH 4.5 solution as indicated (mean ± SEM, n= 20, 22, 10, 6 for control, WT, Q360L, and I271W, respectively).

(C) Averaged and normalized final fluorescence intensity during the last 60 seconds of low pH perfusion (n cells as indicated, mean ± SEM). Paired t-test ***$p < 0.001$.

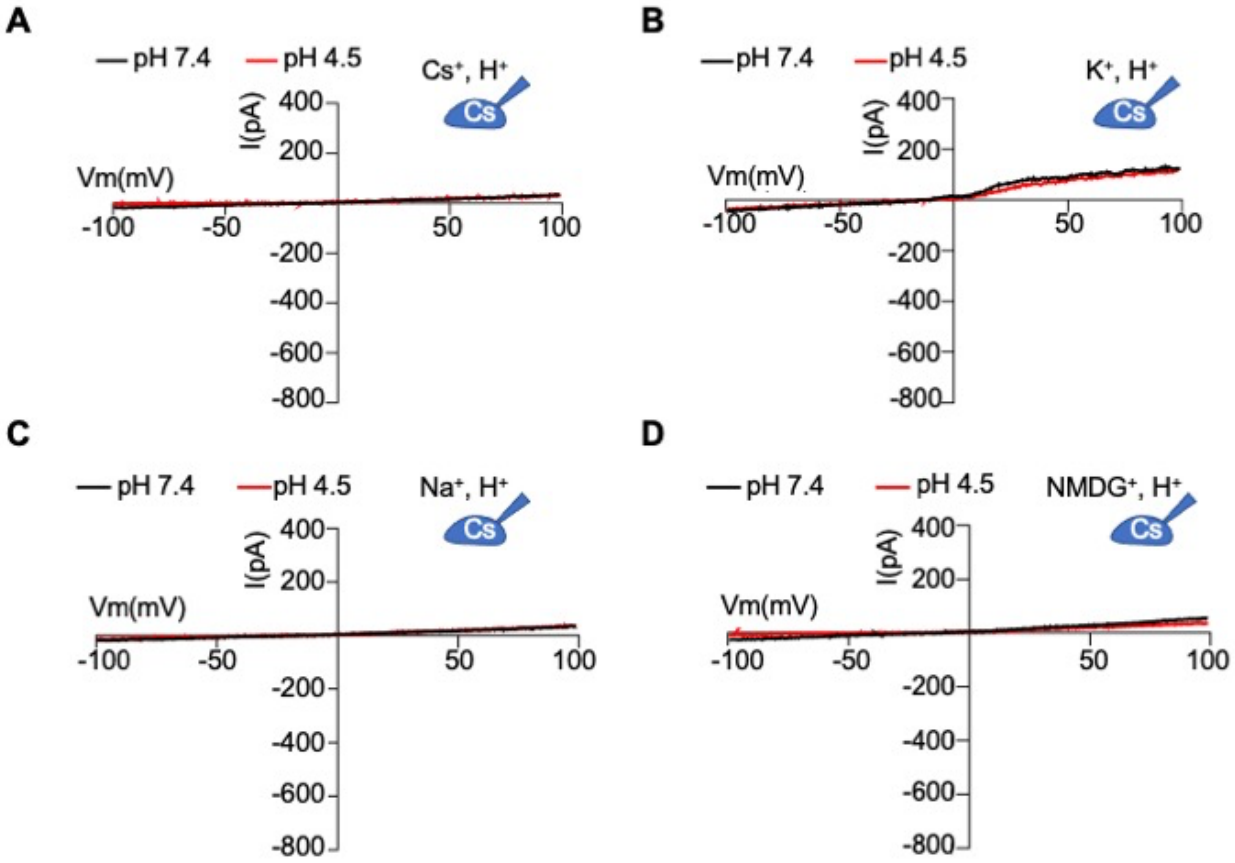

Fig. S3. Controls of electrophysiology recording

(A-D) Representative current-voltage (*I-V*) curves obtained in whole-cell configuration from non-transfected HEK293T cells. The pipette solution contains 150 mM Cs^+. 150 mM Cs^+ (A), 150 mM K^+ (B), 150 mM Na^+ (C), and 150 mM $NMDG^+$ (D) was used in the bath solution, respectively.

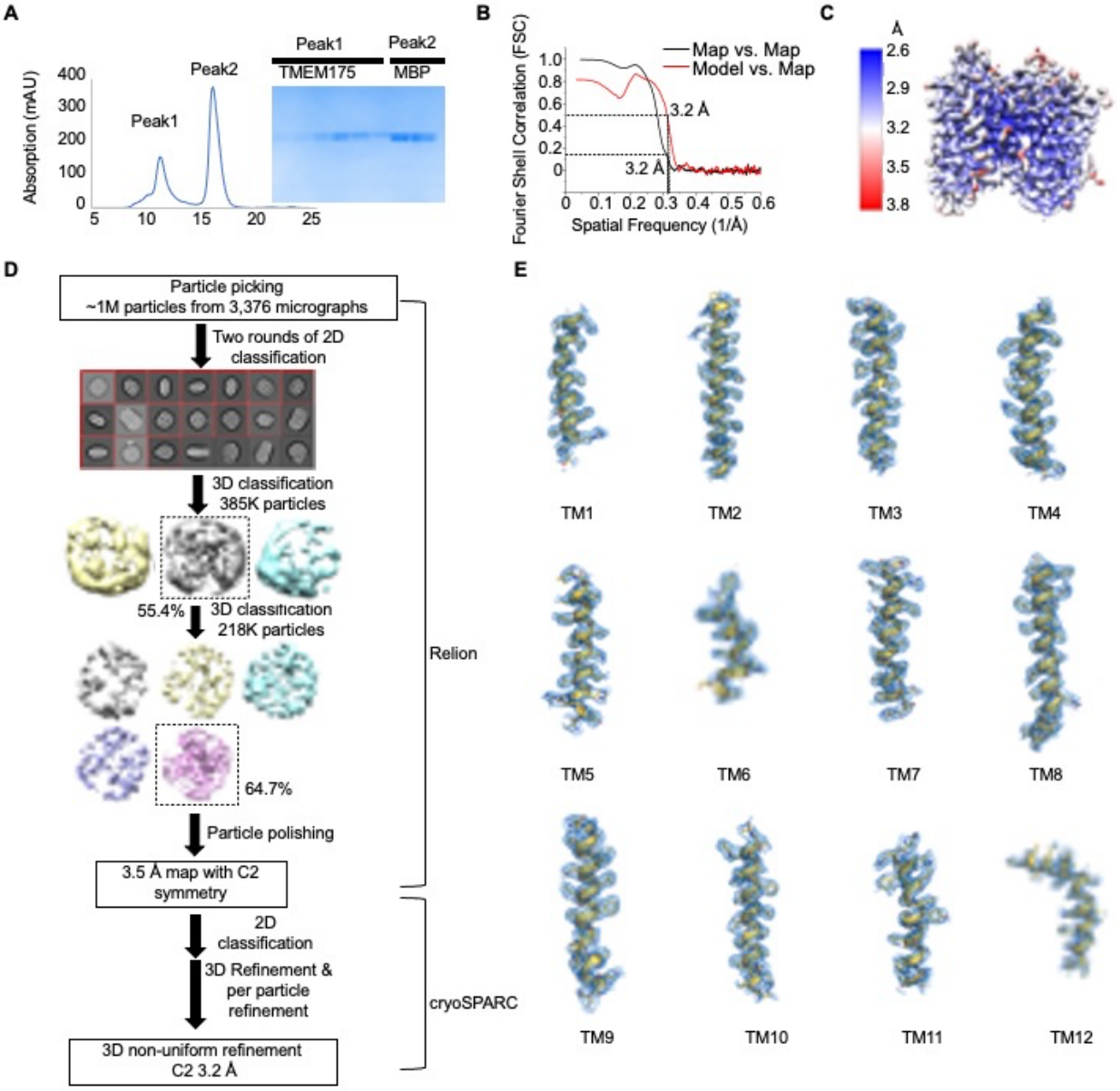

Fig. S4. Purification and reconstruction of human TMEM175
(A) Gel filtration and SDS-PAGE showing purified human TMEM175.
(B) Fourier shell correlation (FSC) curves for 3D reconstruction of human TMEM175 at pH 6.8.
(C) Local resolution map of the reconstruction. The resolution is color-coded as indicated by the scale bar.
(D) Workflow of 3D reconstruction of human TMEM175 at pH 6.8.
(E) The transmembrane segments of the cryo-EM density map fitted with the final atomic model.

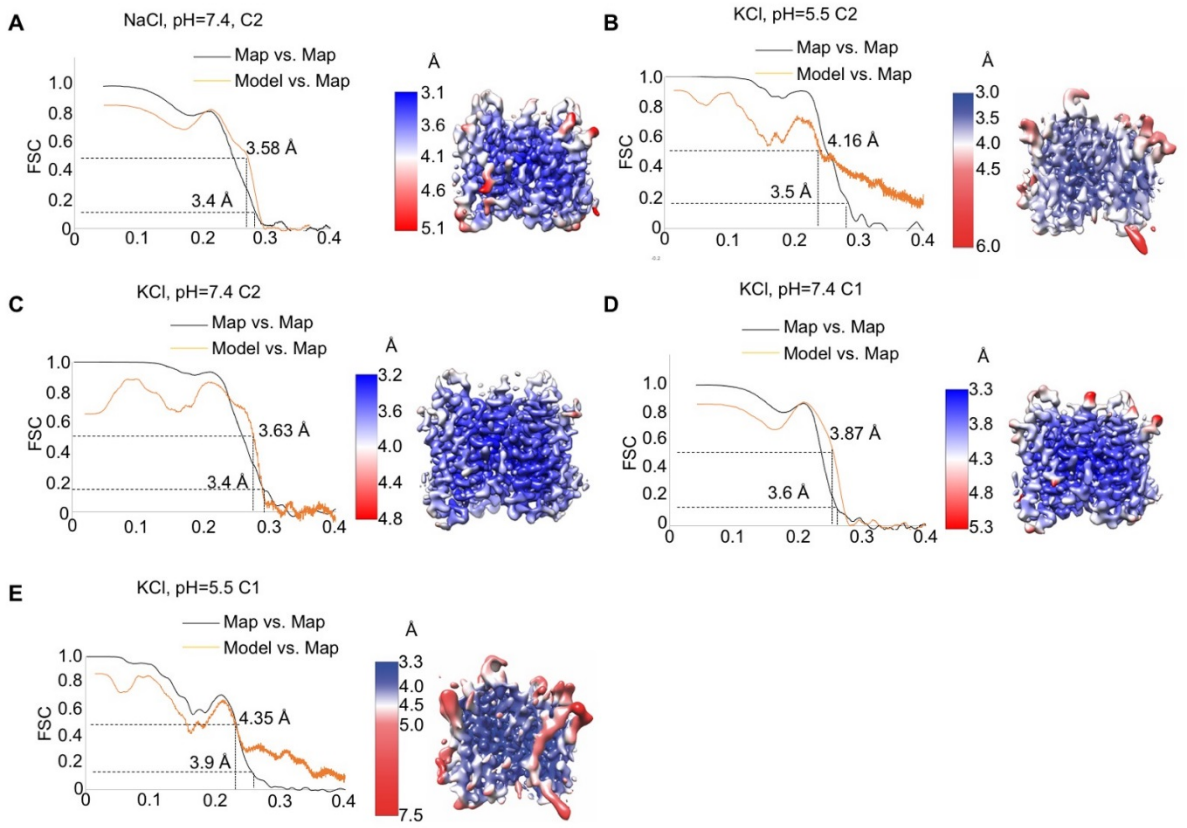

Fig. S5. Reconstruction of human TMEM175 at different pH
(A-E) FSC curves and local resolution maps for 3D reconstruction of human TMEM175 at pH 7.4 in NaCl with C2 symmetry (A), pH 5.5 in KCl with C2 symmetry (B), pH 7.4 in KCl with C2 symmetry (C), pH 7.4 in KCl without symmetry (D), pH 5.5 in KCl without symmetry (E). The resolution is color-coded as indicated by the scale bar.

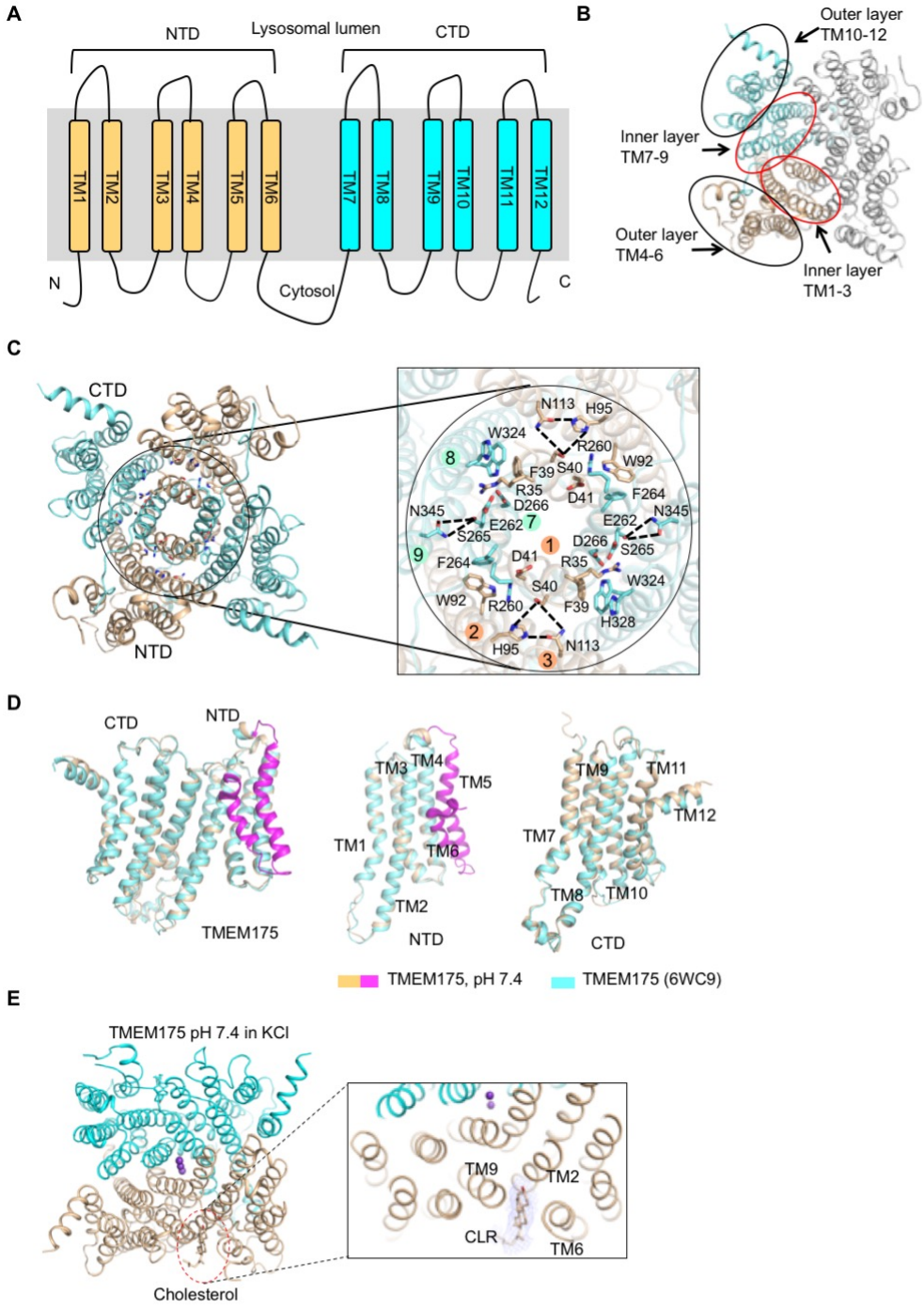

Fig. S6. Assembly and structural comparison of human TMEM175

(A) Two-repeat six-transmembrane topology of human TMEM175.

(B) Dimeric assembly of human TMEM175 with one subunit colored in wheat (NTD) and cyan (CTD) and the other subunit in grey. TM1-3 and TM7-9 constitute an inner layer while TM4-6 and TM10-12 form the outer layer.

(C) Interaction networks mediated by the conserved RxxxFSD motif.

(D) Structure comparison of our human TMEM175 (wheat, pH 7.4) with the published PDB entry 6wc9 (cyan, pH 8.0) (*15*). TM5 and TM6 are highlighted in magenta in our structure and are invisible in 6wc9.
(E) Ribbon diagrams of the human TMEM175 structure at pH 7.4, 150 mM KCl with the two subunits colored in cyan and wheat, respectively. The cholesterol molecule is shown in sticks, interacting with helices 2, 6, 9. Cryo-EM density for the cholesterol is contoured at 1.3 $\boldsymbol{\sigma}$ and shown in gray.

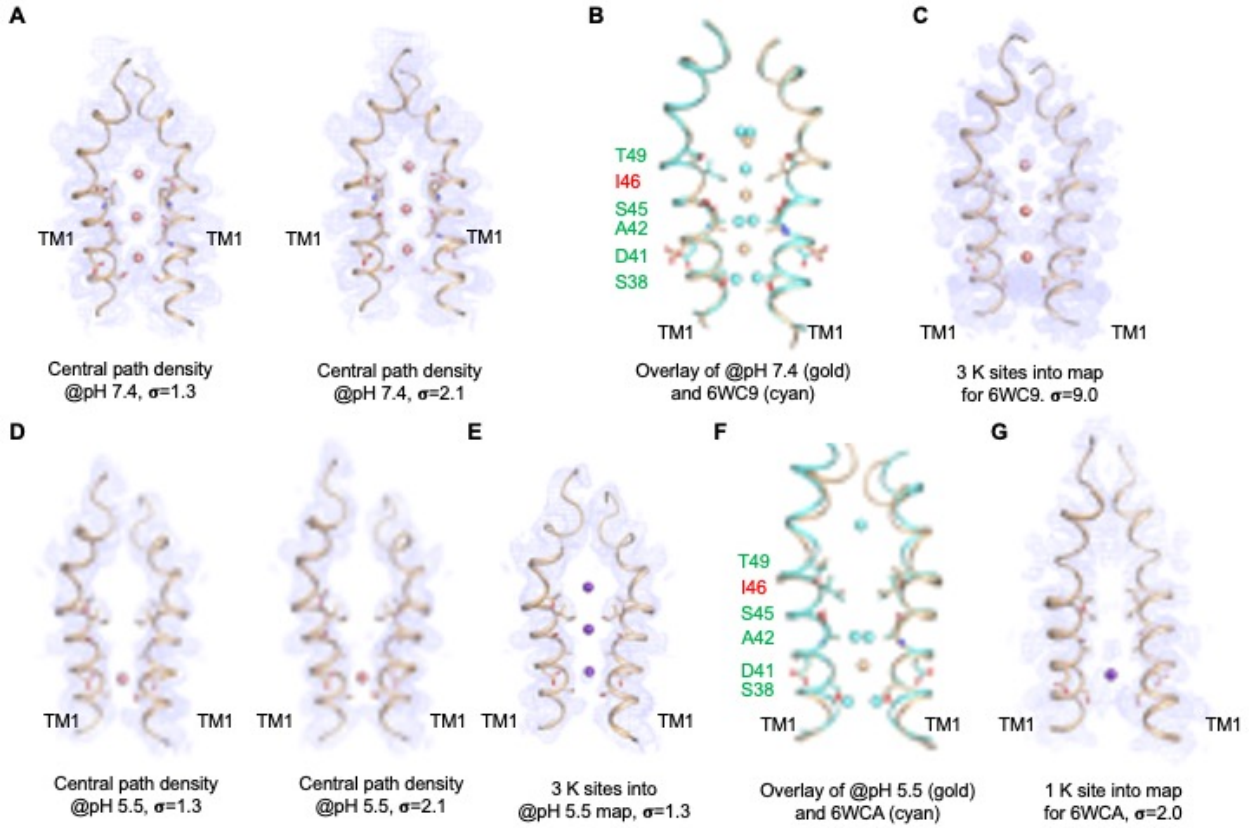

Fig. S7. Structural comparison of TMEM175-KCl at different pH with published open and closed conformation of human TMEM175 structure

(A) Central pore density of pH 7.4 KCl map contoured at 1.3 **σ** and 2.1 **σ** fitted with two TM1 helices and 3 K^+ sites.

(B) Ion permeation pathway comparison between the TMEM175 pH 7.4 KCl structure (wheat) and 6WC9 (cyan) in conformations permeable to K^+. TM1 is shown in ribbon and potassium ions are shown in spheres.

(C) Central pore density of 6WC9 map contoured at 9 **σ** fitted with two TM1 helices and 3 K^+ sites from pH 7.4 KCl structure model.

(D) Central pore density of pH 5.5 KCl map contoured at 1.3 **σ** and 2.1 **σ** fitted with two TM1 helices and 1 K^+ sites.

(E) Central pore density of pH 5.5 KCl map contoured at 1.3 **σ** fitted with two TM1 helices and 3 K^+ sites from pH 7.4 KCl structure model, indicating the unbiased lack of K1 and K2 sites in the pH 5.5 structure.

(F) Ion permeation pathway comparison between the TMEM175 pH 5.5 KCl structure (wheat) and 6WCA (cyan) in conformations impermeable to K^+. TM1 is shown in ribbon and potassium ions are shown in spheres.

(G) Central pore density of 6WCA map contoured at 2.0 **σ** fitted with two TM1 helices and 1 K^+ site from pH 5.5 KCl structure model.

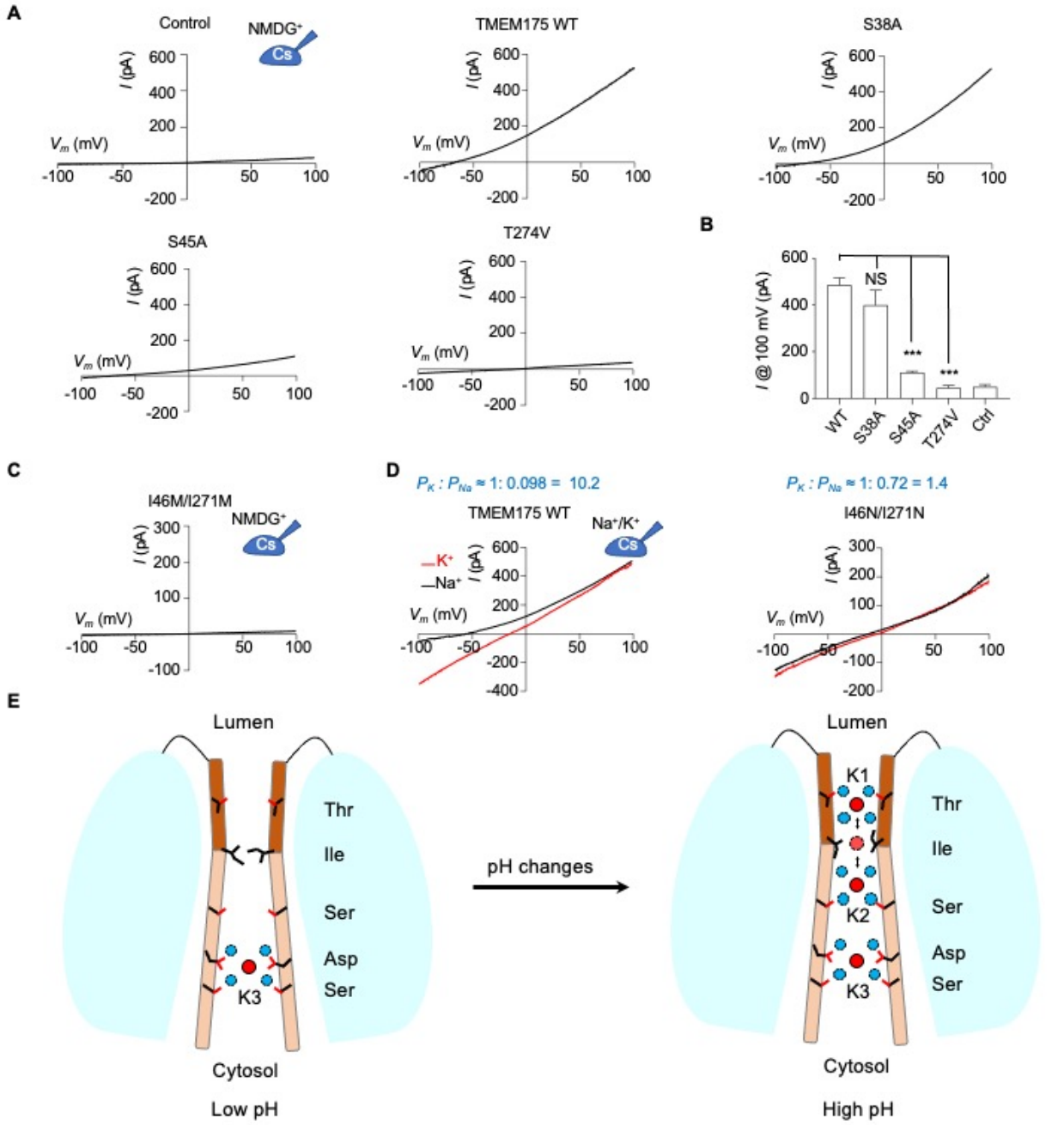

Fig. S8. Cation conductance and selectivity of human TMEM175

(A) Representative current-voltage (*I-V*) curves obtained in whole-cell configuration from HEK293T cells expressing WT *hs*TMEM175 or indicated mutants. Non-transfected cells serve as control (Ctrl). The pipette solution contains 150 mM Cs^+, and 150 mM $NMDG^+$ was used in the bath solution.

(B) Averaged currents at 100 mV (WT, N=4; S38A, N=3; S45A, N=3; T274V, N=4; Ctrl, N=4). Data are presented as mean ± SEM. ***P<0.001; NS, not significant, one-way ANOVA with Dunnet's correction.

(C) A representative *I-V* curve of *hs*TMEM175 I46M/I271M.

(D) Representative *I-V* curves of *hs*TMEM175 WT or double mutant I46N/I271N, showing the ion selectivity for potassium ions over sodium ions. Currents were recorded in whole-cell configuration with 150 mM Cs^+ in pipette solution, and 150 mM Na^+ or K^+ in bath solution.
(E) A model for human TMEM175 gating and K^+ selectivity. pH induced conformational changes and/or potential competition between K+ and protons at acidic pH contribute to the reduced K^+ permeation of TMEM175 at low pH. The hydrophobic gate and the three hydrophilic layers form an integrated functional unit that serves both as a selectivity filter and a restriction gate for human TMEM175. When potassium ions pass through the Ile gate, they undergo dehydration transiently, and the water shell will be regained at the next K^+ site. The difference in dehydration penalty and hydrophilic coordination contribute to the ion selectivity of TMEM175 for K^+ over Na^+.

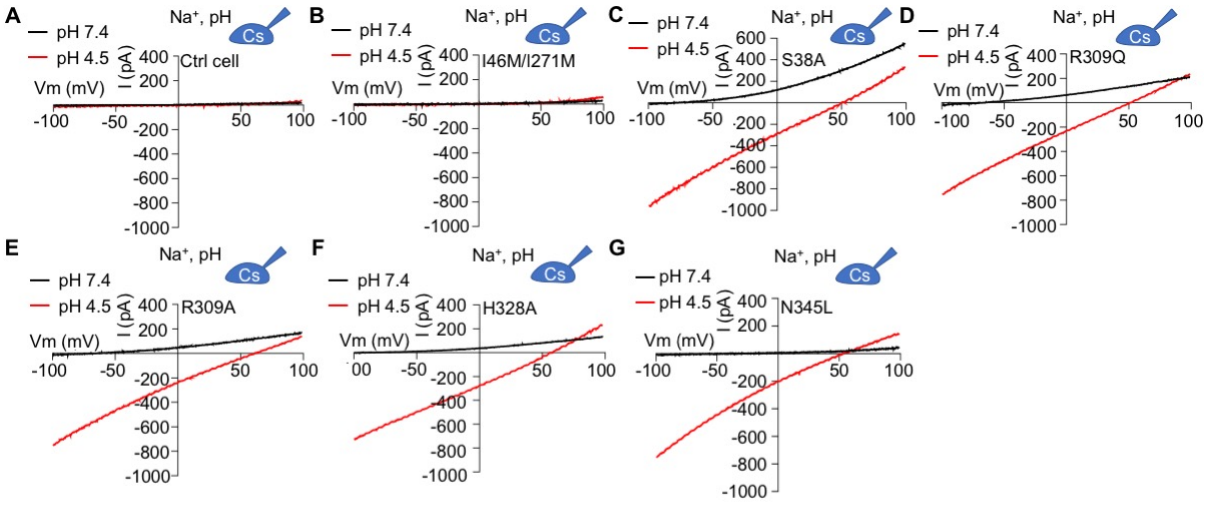

Fig. S9. Mechanisms of proton and potassium ion conductance by human TMEM175
(A-G) Representative *I-V* curves of control cells or cells expressing *hs*TMEM175 mutants I46M/I271M, S38A, R309Q, R309A, H328A, and N345L at pH7.4 and pH 4.5, showing their effects on K^+ and proton conductance, respectively.

Table S1. Cryo-EM Data Collection, Refinement and Validation Statistics

	NaCl, pH 7.4 - HMS (EMDB-21576) (PDB-6W8O)	KCl, pH 7.4 - HMS (EMDB-21577) (PDB-6W8P)	NaCl, pH 6.8 - HMS (EMDB-21575) (PDB:6W8N)	KCl, pH 5.5 (EMDB-23300) (PDB:7LF6)
Data collection & processing				
Magnification	105,000	105,000	105,000	105,000
Voltage (kV)	300	300	300	300
Electron exposure (e/Å^2)	65.02	64.37	67.70	66.5
Defocus range (μm)	-1.0 to -2.7	-1.0 to -2.7	-1.0 to -2.7	-1.0 to -2.7
Pixel size (Å)	0.825	0.825	0.825	0.825
Symmetry imposed	C2	C1/C2	C2	C1/C2
Initial particles (no.)	1,378,039	1,111,591	1,015,093	790,954
Final particles (no.)	145,051	110,220	141,251	117,539
Map resolution (Å) FSC threshold	3.4 0.143	3.6/3.4 0.143	3.2 0.143	3.8/3.5 0.143
Refinement				
Initial model used (PDB code)	5VRE	5VRE	5VRE	5VRE
Model resolution (Å) FSC threshold	3.58 0.5	3.87 0.5	3.20 0.5	4.16 0.5
Model resolution range (Å)	99.3 -3.4	99.3 -3.6	99.3 -3.2	99.3 -3.5
Map sharpening *B* factor (Å^2)	-139	-140	-111	-156
Model composition Non-hydrogen atoms Protein residues Ligands	 6,557 852 N/A	 6,510 844 3	 6,160 804 N/A	 6288 814 N/A
R.m.s. deviations Bond lengths (Å) Bond angles (°)	 0.004 0.748	 0.004 0.765	 0.007 0.766	 0.003 0.710
Validation MolProbity score Clashscore	 2.95 15.33	 3.03 15.11	 2.76 12.62	 1.93 17.02
Ramachandran plot Favored (%) Allowed (%) Disallowed (%)	 91.59 8.41 0.00	 89.59 10.41 0.00	 92.89 7.11 0.00	 96.76 3.24 0.00